

## Tutorial/Article didactique

# Angular momenta dynamics in magnetic and electric field: Classical and quantum approach

**Marcis Auzinsh**

**Abstract:** A standard description of the angular momentum in atomic or molecular physics is based on quantum mechanics. However, especially at large angular-momentum limit in molecules, sometimes a classical approach greatly simplifies problems that are extremely complicated from a quantum-mechanical viewpoint. The aim of this paper is to examine the relationship between the classical and quantum descriptions of the angular-momentum distribution in an ensemble of particles. At first glance, quantum and classical approaches appear to be absolutely different and have very little in common. In this paper this relationship is analyzed. It is shown that similarities can be found between the precession of angular momentum in the external field and the influence of this field upon the wave-function phase of a microparticle. The importance of wave function phases is stressed even for stationary conditions, and some examples of coherent superposition of quantum states are presented. The general method of how to pass from the quantum approach to a classical one is formulated. Results are visualized in the form of 3D distribution functions. This approach allows a graphical interpretation and thus results in a better understanding, sometimes at first glance, of counterintuitive quantum results. As an example the phenomenon of alignment-orientation transition is considered. Rather than presenting only formal derivations, the emphasis is on the instructional aspects, and on illustrating the general approach.

**Résumé :** La description standard du moment cinétique dans les atomes et les molécules fait normalement appel à la mécanique quantique. Cependant, aux grandes valeurs de moment cinétique dans les molécules, l'approche classique simplifie énormément des problèmes qui seraient très complexes en formalisme quantique. Nous examinons ici les relations entre les descriptions classique et quantique du moment cinétique d'un ensemble de particules. À première vue, les deux approches diffèrent dramatiquement et ont très peu en commun. Nous analysons ici cette relation. Nous trouvons une similitude entre la précession (classique) du moment cinétique dans un champ externe et l'influence de ce champ sur la phase de la fonction d'onde de la particule microscopique (quantique). L'importance de la phase est soulignée, même en situation stationnaire et nous présentons quelques exemples de superposition cohérente d'états quantiques. Nous proposons une méthode générale pour passer de l'approche quantique à l'approche classique. Les résultats sont présentés sous la forme de fonctions de distribution 3D. La méthode permet une présentation graphique et ainsi résulte en une meilleure compréhension, parfois très rapide, de certains effets quantiques contre-

Received May 26, 1997. Accepted July 31, 1997.

**M. Auzinsh.**<sup>1</sup> Department of Physics, University of Latvia, 19 Rainis Blvd., Riga ,LV-1586, Latvia and Center for Interdisciplinary Research, University of Bielefeld, Bielefeld, D-33 615, Germany.

<sup>1</sup> Address for correspondence is the Latvian address. **Telephone:** + 371 7227301; **FAX:** + 371 7820113; **e-mail:** mauzins@acad.latnet.lv

intuitifs. Nous développons le cas de la transition alignement–orientation comme exemple. Nous favorisons une présentation pédagogique plutôt que d’insister sur des dérivations formelles.

[Traduit par la rédaction]

## 1. Introduction

Usually when describing angular momentum in atomic or molecular physics, we use a quantum-mechanical approach. However, there are problems, mostly connected with the description of states with large angular-momentum quantum numbers ( $J \sim 10 \dots 100$ ), say, in molecular physics, where the classical approach can obtain reasonably accurate results [1]. Classical equations for large angular momentum are often easier to solve. This makes it possible to treat a whole class of problems, which, from a quantum theory viewpoint, are extremely complicated. For example, one such problem is the interaction of intense laser radiation with molecules in an external electric or magnetic field; see, for example, refs. 2 and 3.

The classical and quantum descriptions of such phenomenon as the well-known Zeeman effect have little in common. On the other hand in general it is obvious that both descriptions must at least in some sense coincide at the limit of large angular momentum. At this point “coincidence of descriptions” does not only mean the coincidence of calculated observable signals. Such coincidence is obvious. It also means the coincidence of how both approaches understand the behavior of particles with a definite angular momentum under well-defined conditions, such as excitation by light with a certain polarization, action of external electric or magnetic fields, etc.

In this paper, we examine the relationship between the quantum and classical descriptions of angular momentum. As examples, Zeeman and Stark effects in atoms and molecules are analyzed. Finally, a general method for interpreting quantum-mechanical results in the large angular-momentum limit from a classical perspective is demonstrated. This general approach is based on the comparison of the quantum density-matrix  $f_{MM'}$  description of angular momentum with the classical angular probability density functions  $\rho(\theta, \varphi)$ . These give a classical characterization of the probability  $dW = \rho(\theta, \varphi)d\Omega$  of finding angular momenta  $\mathbf{J}$  pointing into the solid angle  $d\Omega = \sin\theta d\theta d\varphi$ .

## 2. Magnetic field

### 2.1. Angular-momentum dynamics in a static magnetic field: Classical approach

Let us start our analysis with a simple model. The particle, it must be an atom or a molecule, with angular momentum  $\mathbf{J}$  is placed in an external magnetic field  $\mathbf{B}$  (see Fig. 1). In atomic physics, an angular momentum  $\mathbf{J}$  is always connected with a collinear magnetic moment  $\boldsymbol{\mu}$ . From the viewpoint of classical physics, it can be written as

$$\boldsymbol{\mu} = -\gamma \mathbf{J} \quad (1)$$

where  $\gamma = g_J e/2m$  is a gyromagnetic ratio,  $e$  an electron charge,  $m$  its mass, and the proportionality coefficient  $g_J$  is called the Landé factor [4].

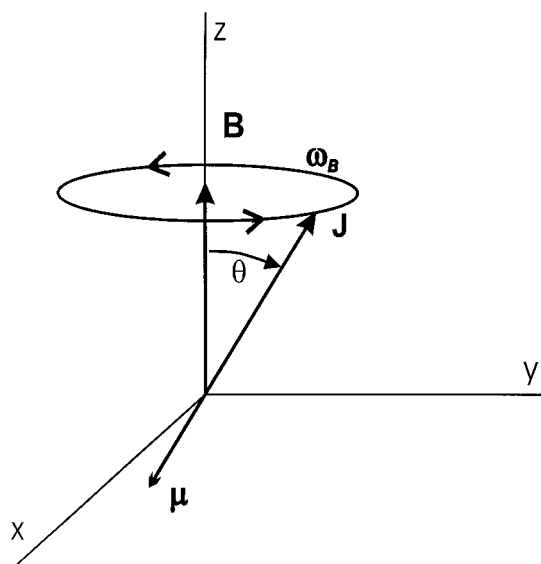
The natural unit for  $J$  in atomic physics is Planck’s constant  $\hbar$  and the natural unit for the atomic magnetic moment is the Bohr magneton  $\mu_B = e\hbar/2m$ .

The interaction between the magnetic moment of the particle and the external field causes a torque,

$$\mathbf{M} = \boldsymbol{\mu} \times \mathbf{B} \quad (2)$$

to which the angular momentum will be subjected,

$$d\mathbf{J}/dt = \mathbf{M} \quad (3)$$

**Fig. 1.** Precession of an angular momentum in an external magnetic field

The result of the action of torque will be the precession of the angular momentum with angular velocity

$$\omega_B = \frac{gJ\mu_B B}{\hbar} \quad (4)$$

During this precession, the angle  $\theta$  between the angular momentum  $\mathbf{J}$  and the magnetic field  $\mathbf{B}$  is constant. The angular velocity of the precession is independent of this angle (contrary to the particle in an external electric field, as will be shown later).

However, in the microworld, we usually do not have the possibility of investigating a single particle. In most cases we deal with an ensemble of particles determined by experimental conditions.

Let us consider such an ensemble of gaseous molecules prepared by a laser pulse that excites a resonant transition in an external magnetic field  $\mathbf{B}$ . Laser radiation is linearly polarized with light  $\mathbf{E}$ -vector along the  $y$  axis as shown in Fig. 2a.

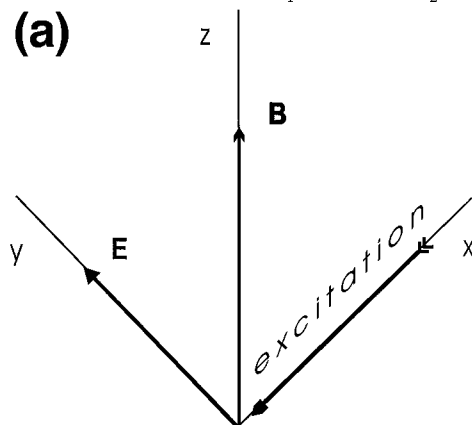
At the beginning, let us assume that the laser pulse is short in comparison with the precession period  $T_B = 2\pi/\omega_B$ , and the excited molecular state decays slowly in comparison with both, the laser impulse duration and the precession period,  $T_B$ , of the molecule. If during the excitation the molecule undergoes a transition in which the angular-momentum quantum number of the initial state  $J''$  is equal to the angular-momentum quantum number of the excited state  $J'$ , a so-called  $Q$ -type transition [5], then in the classical approach, the transition dipole moment is parallel to the angular momentum of molecules  $\mathbf{J}$  [1,6]. In the classical approach, the transition dipole moment is the dipole that starts oscillating as a result of absorption and emits an electromagnetic field during radiation.

Immediately after the laser pulse, the classical probability density  $\rho(\theta, \varphi)$  of finding molecules in the excited state with their angular momentum in the direction  $(\theta, \varphi)$  is characterized by a dumbbell-shaped function spanning along the  $y$  axis (see Fig. 2b(1))

$$\rho(\theta, \varphi, t) = \sin^2 \theta \sin^2(\varphi - \omega_B t) \quad (5)$$

As in classical physics, the absorption probability is proportional to the cosine of the angle between the laser-light polarization vector  $\mathbf{E}$  and the absorbing dipole squared, this is an obvious

**Fig. 2.** Ensemble of molecules excited by a light pulse in a magnetic field; (a) the geometry of the excitation, (b) (see facing page) 1 –  $\omega_B t = 0$ ; 2 –  $\omega_B t = \frac{\pi}{4}$ ; 3 –  $\omega_B t = \frac{\pi}{2}$ ; 4 –  $\omega_B t = \frac{3\pi}{4}$ ; 5 –  $\omega_B t = \pi$ ; 6 –  $\omega_B t = \frac{5\pi}{4}$ .



result, especially if we remember that we consider the  $Q$ -type transition with a transition dipole to be parallel to the angular momentum.

Now, when looking at the time evolution of this distribution after the laser pulse, we have the precession of this distribution around the magnetic field  $\mathbf{B}$ . The important point is that all angular momenta precess with the same angular frequency  $\omega_B$ , and as a result, the shape of the distribution apart from the rotation will remain unchanged (see Fig. 2b). Taking into account the radiation decay of the state (not included in (5) and Fig. 2b), the size of distribution will decrease in time, still preserving its shape.

If we detect the fluorescence intensity with a chosen linear polarization from such an ensemble, we observe the well-known quantum beats [7], the effect that in the quantum approach is attributed to the interference of quantum states.

As a second example, we analyze the excitation of molecules with continuous laser radiation. The geometry of experiment and transition types is the same as in the previous case.

Now, the most interesting case is when the lifetime of the excited state and the precession period are comparable. In the limit where the precession is slow, the molecule returns to the ground state before the angular momentum manages to turn around  $\mathbf{B}$  by a substantial angle. As long as we are depicting the angular-momentum distribution in the excited state, we will have the distribution function  $\rho(\theta, \varphi)$  as shown in Fig. 3(1).

At the other limit, the precession frequency  $\omega_B$  will be much higher than the decay rate  $\Gamma$  of the excited molecules. Consequently, the angular momentum of the molecules will precess around  $\mathbf{B}$  many times before it decays. This leads to the function  $\rho(\theta, \varphi)$  in the form shown in Fig. 3(4). In intermediate cases (Figures 3(2) and 3(3)), we are in between these two extremes. Figs. 3(2) and 3(3) illustrate the situation, when by increasing the magnetic field and with it the precession rate, we increase the angle through which the angular momentum manages to turn before decay.

To obtain the explicit form of  $\rho(\theta, \varphi)$  for the arbitrary magnetic field strength, we must multiply (5) by a factor  $\exp(-\Gamma t)$  that accounts for the decay of the excited state at rate  $\Gamma$  and average  $\rho(\theta, \varphi, t)$  in time. As a result, we then have

$$\rho(\theta, \varphi) = \frac{1}{2} \sin^2 \theta \left( \frac{1}{\Gamma} - \frac{\Gamma \cos 2\varphi + 2\omega_B \sin 2\varphi}{\Gamma^2 + 4\omega_B^2} \right) \quad (6)$$

(b)

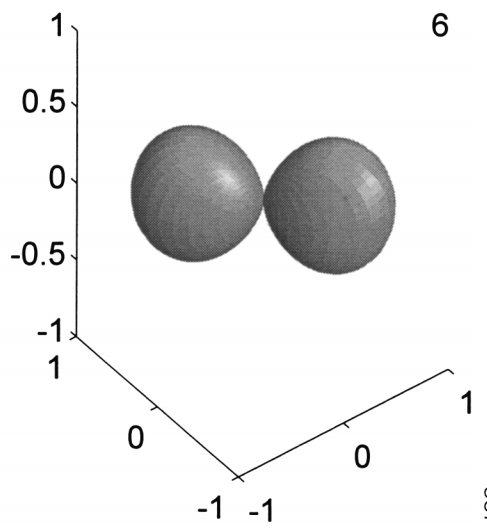
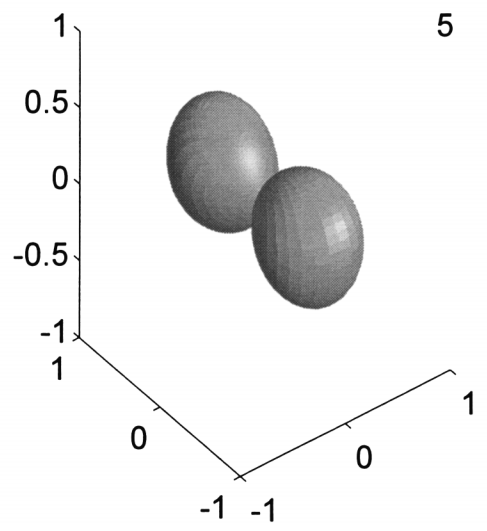
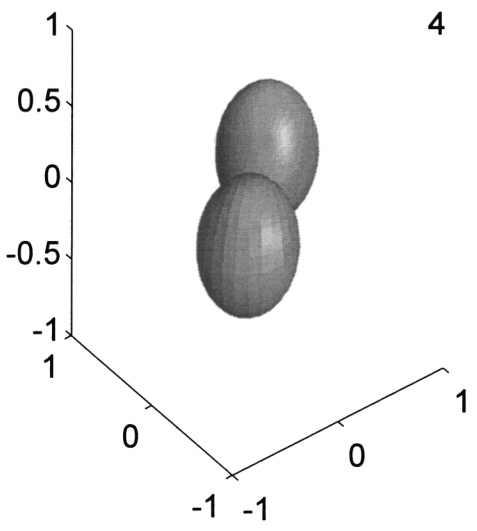
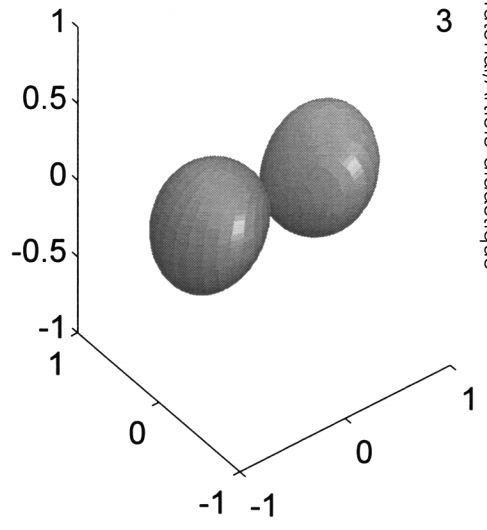
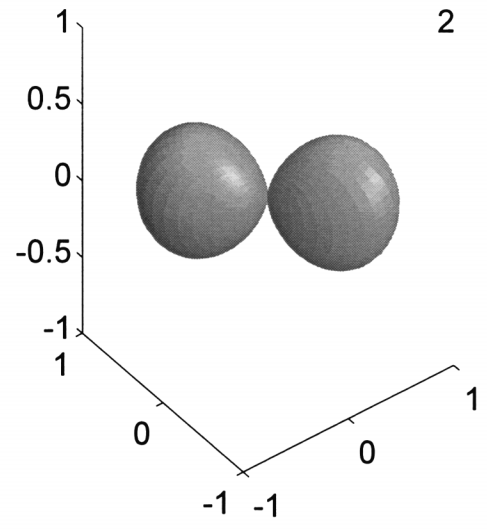
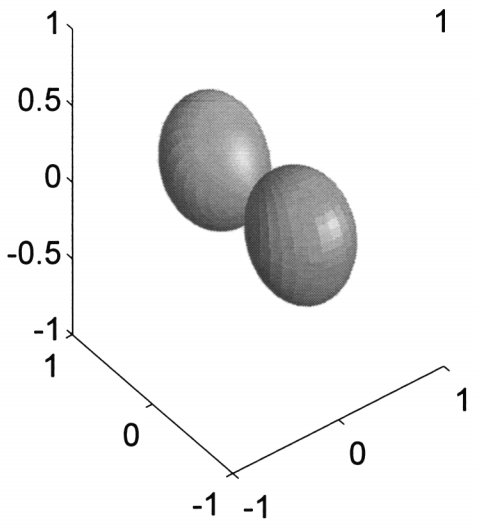
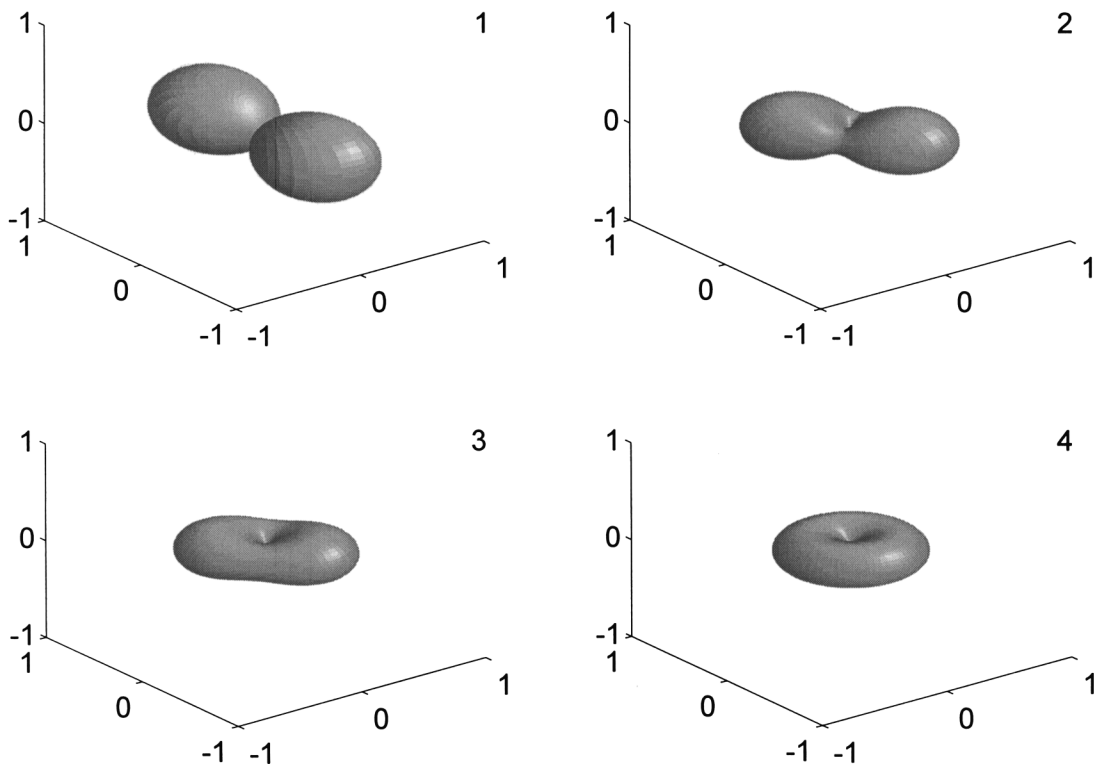


**Fig. 3.** Ensemble of molecules excited by a continuous radiation in magnetic field; 1 –  $\omega_B/\Gamma = 0$ ; 2 –  $\omega_B/\Gamma = 1.0$ ; 3 –  $\omega_B/\Gamma = 2.5$ ; 4 –  $\omega_B/\Gamma = \infty$ .



## 2.2. Angular-momentum dynamics in the magnetic field: Quantum-mechanical approach

In a quantum-mechanical description, particles in a state with angular-momentum quantum number  $J$  exposed to an external magnetic field  $B$  gain an additional energy

$$E_M = g_J \mu_B M_J B \quad (7)$$

depending linearly not only on the magnetic field strength, but also on the magnetic quantum number  $M_J$ , which can assume discrete values in the range from  $-J$  to  $J$ . In quantum mechanics, the angular-momentum quantum number  $J$  defines the modulus of the angular momentum

$$|J| = \sqrt{J(J+1)} \hbar \quad (8)$$

but the magnetic quantum number  $M_J$  its discrete projection on the magnetic field direction (or quantization axis  $z$ )

$$J_Z = M_J \hbar, M_J = -J, -J+1, -J+2 \dots J \quad (9)$$

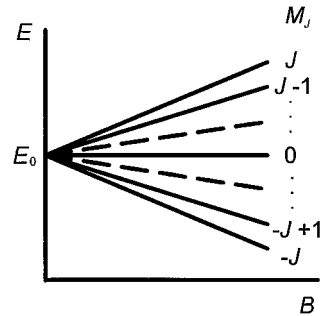
As a result, in an external magnetic field, according to quantum mechanics, energy levels with initial energy  $E_0$  split into  $2J+1$  components, see Fig. 4.

At first glance, classical and quantum descriptions of particles with angular momentum in an external magnetic field have little in common, but even at this stage we can find some similarities.

In quantum angular-momentum theory, each quantum state corresponding to a magnetic sublevel is characterized by the stationary wave function  $Y_{JM}$  [8,9]. If we add the phase factor in a standard form, we obtain the total wave function for each particular state in the form

$$\Psi_{JM}(t) = Y_{JM} e^{-i[(E_0+E_M)/\hbar]t} \quad (10)$$

**Fig. 4.** Magnetic sublevel structure for a particle in a magnetic field.



where  $E_0$  is the energy of the state in the absence of the magnetic field.

In the following, it is important to remember that by turning a system of coordinates around  $B$  by an angle  $\varphi$ , the stationary wave function acquires an additional phase according to

$$Y_{JM_J} = Y'_{JM_J} e^{-iM_J\varphi} \tag{11}$$

where  $Y_{JM_J}$  is a function in the final system of coordinates, whereas  $Y'_{JM_J}$  is a function in the initial system of coordinates [8,9].

Now, if we compare the phase factor in (10) connected with the additional energy (7) of the quantum state in the magnetic field with the phase that the wave-function gains under the rotation

$$-iM_J\varphi = \frac{-i g_J \mu_B B M_J t}{\hbar} \tag{12}$$

then we obtain the angular velocity of the “precession” of the wave-function in an external magnetic field

$$\omega_B = \frac{\varphi}{t} = \frac{g_J \mu_B B}{\hbar} \tag{13}$$

As we can see, it is exactly the same velocity that we obtain from the classical approach, see (4).

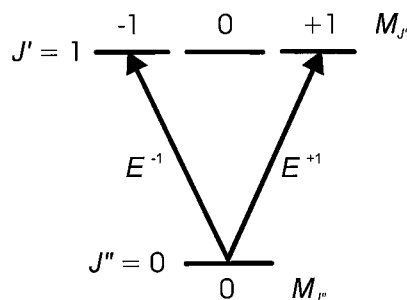
At first glance, the last result seems to make no sense because the probability density  $|Y_{JM}|^2$  for each  $|JM\rangle$  state is axially symmetric and precession around the symmetry axis (magnetic field  $B$ ) has no effect on this distribution [1,8,9]. This attitude can be supported by the feeling that we sometimes get from quantum mechanics textbooks, that in a stationary case, the wave-function phase has no influence on the observable results. Actually, the situation is different. In experiments, we usually excite the *coherent superposition* of quantum states. This concept is extremely important in modern quantum theory. As an example, let us consider the optical excitation of the  $J'' = 0 \rightarrow J' = 1$  transition in the geometry as depicted in Fig. 2a.

In this geometry, the unit light polarization vector [1,9] has the following components in a cyclic coordinate system that is most convenient for the angular-momentum theory:

$$\begin{aligned} E^{+1} &= -(1/\sqrt{2})(E_x - iE_y) = i/\sqrt{2} \\ E^0 &= E_z = 0 \\ E^{-1} &= (1/\sqrt{2})(E_x + iE_y) = i/\sqrt{2} \end{aligned} \tag{14}$$

This means that from a single ground-state sublevel  $|J'' = 0, M_{J''} = 0\rangle$  optical transition occurs simultaneously to two excited state sublevels, namely,  $|J' = 1, M_{J'} = -1\rangle$  and  $|J' = 1, M_{J'} = +1\rangle$ , see Fig. 5. This means that these sublevels are excited coherently, and synchronization between the phases of the respective wave functions is established.

Fig. 5. Optical transitions between magnetic sublevels at the geometry of excitation depicted in Fig. 2a.



Keeping in mind that both transitions depicted in Fig. 5 have the same probability [1] (in general characterized by the respective Clebsch–Gordan coefficient), the total wave function of an excited state in the case of a short exciting pulse can be written as

$$\Psi_{J'}(t) = e^{-i(E_0/\hbar)t} \left( \frac{i}{\sqrt{2}} Y_{1-1} e^{-i(E_{-1}/\hbar)t} + \frac{i}{\sqrt{2}} Y_{11} e^{-i(E_1/\hbar)t} \right) \quad (15)$$

Inserting the  $Y_{1\pm 1}$  functions in (15) in the explicit form  $Y_{1\pm 1} = \mp \frac{1}{2} \sqrt{\frac{3}{2\pi}} \sin \theta e^{\pm i\varphi}$  [1, 8, 9] and calculating the quantum-mechanical probability density  $|\Psi_{J'}(t)|^2$  for this example, we can get once more for particles in an external magnetic field (7) a dumb-bell-shaped quantum-mechanical probability density distribution that precesses in the magnetic field

$$|\Psi_{J'}(t)|^2 \sim \sin^2 \theta \sin^2(\varphi - \omega_B t) \quad (16)$$

where  $\omega_B$  is the same precessional frequency we get from the classical description, see (4).

This result raises the following question: how can a quantum state have a preferred direction in an  $xy$  plane? We know from quantum angular-momentum theory, that all angular-momentum operator eigenstates are axially symmetric [9]. This is a direct result of the Heisenberg uncertainty relation  $\Delta J_z \Delta \varphi \geq \hbar/2$ . It tells us that if we know the angular-momentum projection  $J_z = M\hbar$  we cannot specify the other two projections  $J_x$  and  $J_y$  determined by the angle  $\varphi$ . Is the Heisenberg uncertainty relation violated here? The answer is — no. In this example, we do not have a pure operator eigenstate, but coherent superpositions of the states, see (15) with two different  $J_z$  projections. So we bring uncertainty into  $J_z$  because the particle is simultaneously in two  $M_J$  states. This allows us to obtain a quantum state with a preferred direction in the  $xy$  plane. Such superpositional states are often used in quantum chemistry. For example, orbitals of the type  $p_x = -(1/\sqrt{2})(p_{+1} - p_{-1})$  are known to be “dumb-bells” stretched along the  $x$  axis [10]. For superpositional states it is typical to have nonaxially symmetric distribution in the  $xy$  plane [1, 2].

The main difference between (5) and (16) is that (5) is a classical *angular-momentum* distribution, but (16) is a quantum angular distribution of *electrons* in the case of atoms, or *molecular axes* in the case of diatomic or linear molecules. In some sense, these distributions must be “orthogonal” because the molecular axes are almost perpendicular to their angular momenta. The reason why we get distributions of the same shape in both classical and quantum examples is that in the classical case we analyzed the  $Q$ -type transition ( $J' - J'' = 0$ ) where the transition dipole moment is parallel to  $\mathbf{J}$ , whereas in the quantum example we analyzed the  $R$ -type transition ( $J' - J'' = 1$ ), where in the classical limit the transition dipole moment is known to be perpendicular to  $\mathbf{J}$  [1, 6].

As a second example in the quantum approach, we consider once more the Hanlé-effect type experiment [11]. Let us suppose the same geometry of excitation and type of transition as in the



previous case (see Fig. 5), but the excitation is by continuous wave radiation in this case. In addition, we assume that the excited state has a definite decay rate  $\Gamma$ . All we must do to obtain the quantum-mechanical probability density for this case is, first, to multiply  $\Psi_{J'}$  in the form of (15) by  $e^{-(\Gamma/2)t}$  to account for the decay of the excited state. As a result, we need to multiply (16) by  $e^{-\Gamma t}$  and to account for a stationary excitation to average (16) over time. After doing this we get

$$|\overline{\Psi_{J'}}|^2 \sim \sin^2 \theta \left( \frac{1}{\Gamma} - \frac{\Gamma \cos 2\varphi + 2\omega_B \sin 2\varphi}{\Gamma^2 + 4\omega_B^2} \right) \quad (17)$$

Again, it is a distribution of precisely the same shape as the one depicted in Fig. 3. With respect to the comparison of classical and quantum probability densities, we can make all the same comments about it as we did in the previous example.

One remarkable point with the quantum examples is that we will get exactly the same molecular-axis distribution for the  $R$ -type transition as for large  $J$  in classical theory. This happens very often (but not always) if we do not consider a single quantum state, but a superposition of states that can be created in a real experiment; then quantum and classical probability densities fully coincide not only at the large  $J$  limit but also at very small  $J$ , as is the case in this example.

### 3. Electric field

#### 3.1. Angular-momentum dynamics in electric field: Classical approach

The classical approach to the description of the behavior of particles with angular momentum  $\mathbf{J}$  in a static electric field (Stark effect) is considerably less well known. Sometimes, one can even read in physics textbooks that the Stark effect is a purely quantum effect and that does not have a classical model.

Despite these statements, in a recent publication by Hilborn [12], we can find the classical description of the precession of the angular momentum of particles in an external electric field. It can be seen from ref. 12 that in the geometry in Fig. 1 that where the magnetic field  $\mathbf{B}$  is replaced by an electric field  $\mathcal{E}$  the angular momenta  $\mathbf{J}$  of particles possessing the quadratic Stark effect (common for most atoms and rotating diatomic and linear molecules) precess around  $\mathcal{E}$  with an angular frequency

$$\omega_{\mathcal{E}} = C \frac{\mathcal{E}^2 d \cos \theta}{J} \quad (18)$$

where  $d$  is the permanent dipole moment of the particles (that must be replaced with  $\Delta\alpha$  — electric polarizability anisotropy if the particles have  $d = 0$ ),  $\mathcal{E}$  is the electric-field intensity, and  $C$  is the proportionality coefficient. It can be seen that in this case the precession frequency depends on the angle  $\theta$ , see Fig. 1, and when  $\cos \theta$  changes sign at  $\theta = \pi/2$ , the angular momentum changes the direction of the precession.

This leads to very unusual dynamics for the ensemble of angular momentum in the external field. Let us consider the same example in the case of a magnetic field, namely, pulsed optical excitation in a  $Q$ -type transition molecular state without decay. The result of the calculation in the classical approach, based on the absorption probability dependence on spherical angles  $\theta$ ,  $\varphi$ , and (18), is

$$\rho(\theta, \varphi, t) = \sin^2 \theta \cdot \sin^2 (\varphi + \tilde{\omega}_{\mathcal{E}} \cos \theta \cdot t) \quad (19)$$

where we singled out the  $\cos \theta$  dependence from  $\omega_{\mathcal{E}} = \tilde{\omega}_{\mathcal{E}} \cos \theta$ . Depicting the  $\rho(\theta, \varphi)$  evolution in time graphically, we obtain Fig. 6.

It is clearly seen from Fig. 6 that the angular momentum with opposite projection on the electric field  $\mathcal{E}$  precesses in the opposite direction and the precession velocity also depends on the absolute value of this projection. It leads to the situation that the angular-momentum distribution spreads out in time. The dynamics of an ensemble of particles in an electric field is totally different from the

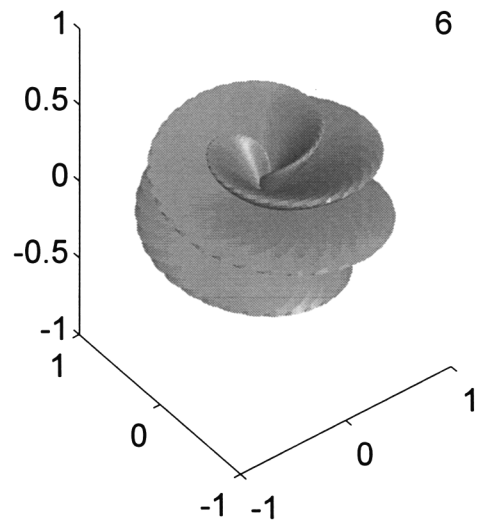
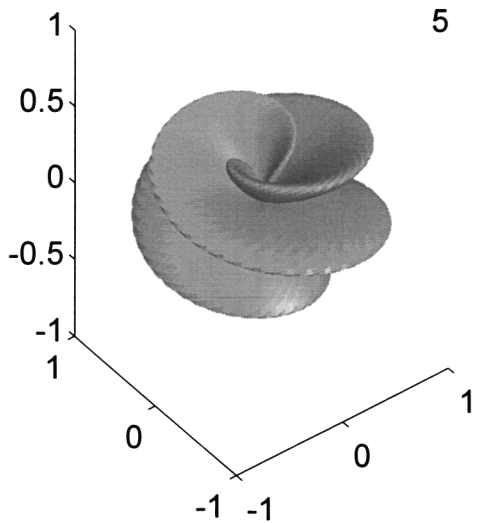
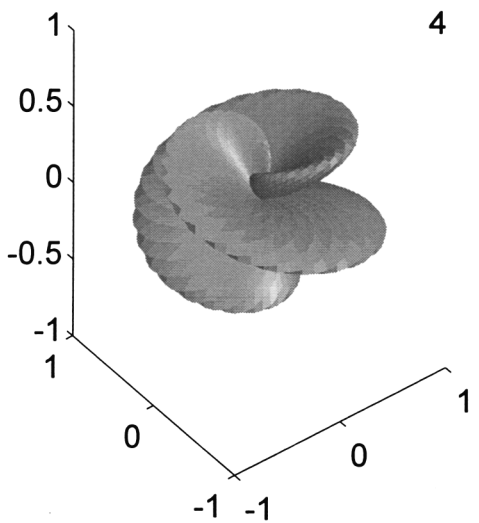
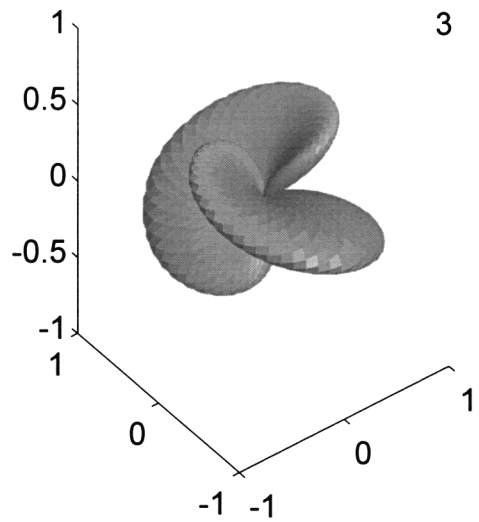
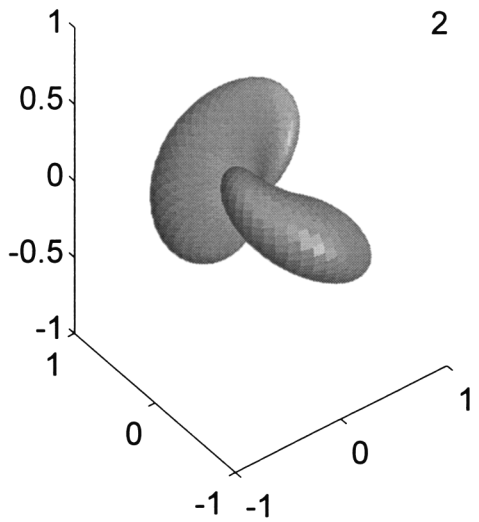
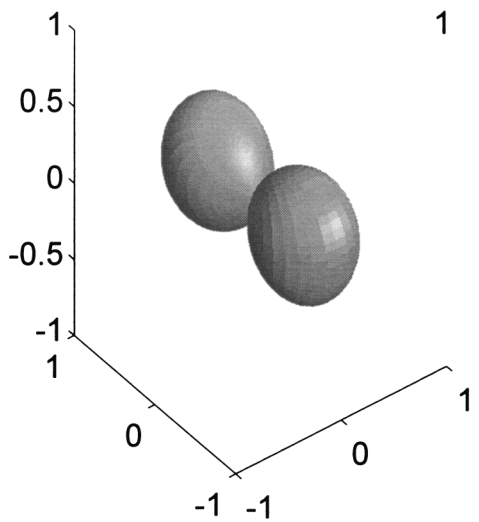
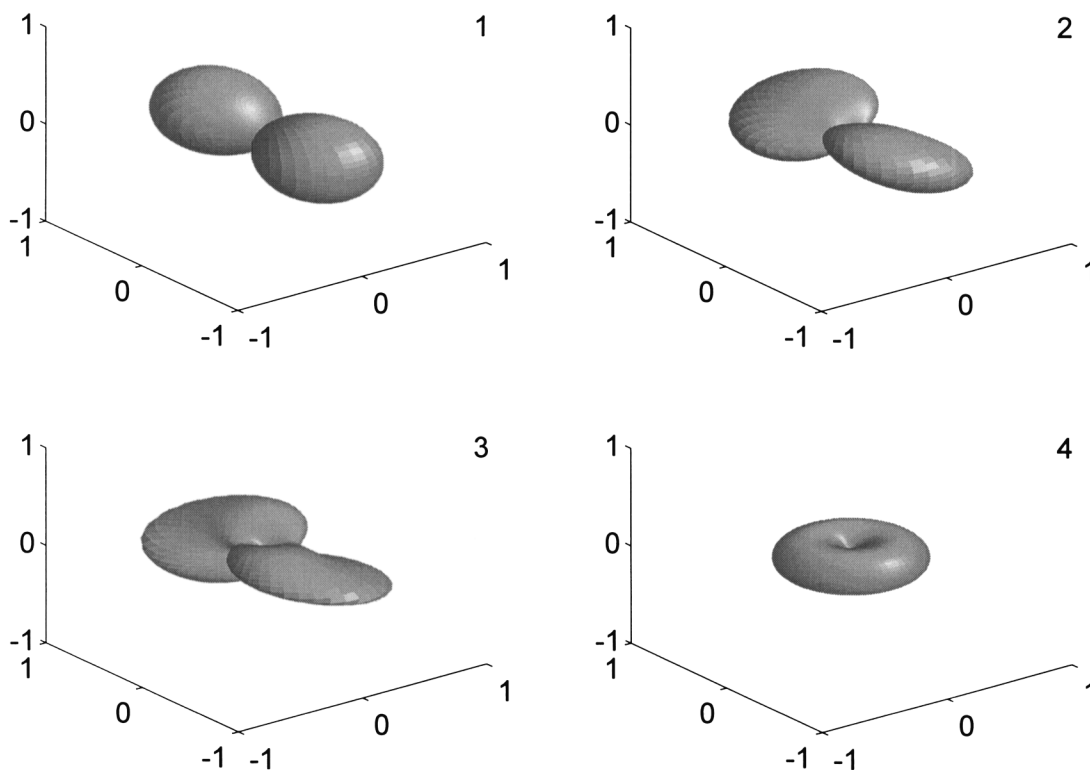


**Fig. 7.** Ensemble of molecules excited by continuous radiation in electric field; 1 –  $\omega_\varepsilon/\Gamma = 0$ ; 2 –  $\omega_\varepsilon/\Gamma = 1.0$ ; 3 –  $\omega_\varepsilon/\Gamma = 2.5$ ; 4 –  $\omega_\varepsilon/\Gamma = \infty$ .



dynamics of the corresponding ensemble in a magnetic field. In an electric field, we cannot expect to observe a quantum beat signal in fluorescence of the type we discussed in Sect. 2.1.

In the following example, we consider the same experimental geometry and transition type, but with a continuous wave excitation and a state decaying with rate  $\Gamma$ . To obtain an angular-momentum distribution all we need to do is multiply (19) by an exponential factor  $e^{-\Gamma t}$  and find a time average of the result.

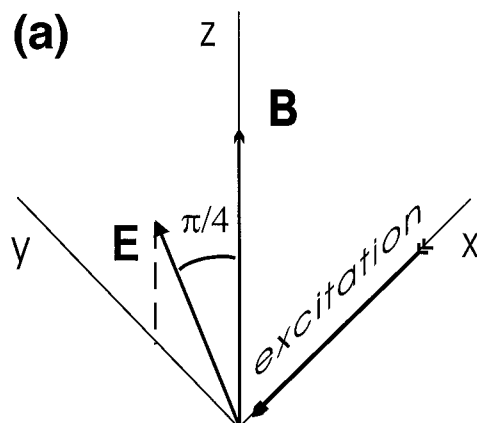
After performing this procedure we obtain

$$\varphi(\theta, \varphi) = \frac{1}{2} \sin^2 \theta \left( \frac{1}{\Gamma} - \frac{\Gamma \cos 2\varphi - 2\tilde{\omega}_\varepsilon \sin 2\varphi \cos \theta}{\Gamma^2 + 4\tilde{\omega}_\varepsilon^2 \cos^2 \theta} \right) \quad (20)$$

This probability density represents the Stark analog to the Hanlé effect analyzed in Sect. 2.1. In Fig. 7, this probability density is presented for four different  $\chi = 2\tilde{\omega}_\varepsilon/\Gamma$  values.

**Fig. 6.** (See facing page.) Ensemble of molecules excited by a light pulse in electric field; 1 –  $\omega_\varepsilon t = 0$ ; 2 –  $\omega_\varepsilon t = \frac{\pi}{2}$ ; 3 –  $\omega_\varepsilon t = \pi$ ; 4 –  $\omega_\varepsilon t = \frac{3\pi}{2}$ ; 5 –  $\omega_\varepsilon t = 2\pi$ ; 6 –  $\omega_\varepsilon t = \frac{5\pi}{2}$ .

**Fig. 8.** “Stark” quantum beats; (a) the geometry of the excitation; (b) (see facing page)  $1 - \omega_s t = 0$ ;  $2 - \omega_s t = 0.4\pi$ ;  $3 - \omega_s t = 0.5\pi$ ;  $4 - \omega_s t = \pi$ ;  $5 - \omega_s t = 1.5\pi$ ;  $6 - \omega_s t = 2\pi$ ;



### 3.2. Angular-momentum dynamics in an electric field: The quantum-mechanical approach

In the quantum approach, microparticles exhibiting a quadratic Stark effect in an external electric field gain an additional energy

$$E_M = \tilde{\omega}_0 \hbar [J(J+1) - 3M^2] \mathcal{E}^2 \quad (21)$$

This formula shows that the additional energy depends on  $\mathcal{E}^2$  and  $M^2$ , i.e., at given  $\mathcal{E}$ , quantum sublevels are no longer equidistant as they were in the magnetic field, see Fig. 4. Besides, states  $M$  and  $-M$  have the same energy at any electric field strength, that is, states with  $M \neq 0$  are doubly degenerated.

Performing the same manipulations as in the case of the magnetic field (see Sect. 2.1) to associate this gain of additional energy with the “precession” frequency of the respective wave function in an external electric field, we have

$$-iM_J \varphi = -i\tilde{\omega}_0 [J(J+1) - 3M_J^2] \mathcal{E}^2 t \quad (22)$$

This is the analog to expression (12).

If we are only interested in the relative precession frequency, we can keep only the  $M$ -dependent part in the right-hand side of (22). This leads to

$$\omega_\varepsilon = \varphi/t = \tilde{\omega}_0 3M_J \mathcal{E}^2 \quad (23)$$

which once more coincides in the same way with the frequency of angular precession in a classical approach as in the case of the magnetic field, see (18). This coincidence becomes very clear if we remember that in the vector model of quantum angular momentum we have  $M_J/\sqrt{J(J+1)} = \cos \theta$  [8].

Let us have a brief look at some examples where this precession of wave functions exhibits itself through the evolution of a coherent superposition of quantum states. We analyze once again a  $J'' = 0 \rightarrow J' = 1$  optical transition caused by a linearly polarized light. However, the geometry of excitation must be chosen with more sophistication than in the case of the magnetic field. In the magnetic field geometry (Fig. 2a), we coherently excited  $|1 - 1\rangle$  and  $|1 - 1\rangle$  magnetic sublevels (Fig. 5) and then we actually examined “beats” between the phases of these wave functions. There will be no beats between these states in the electric field, because they have the same energy and are degenerated.

**(b)**

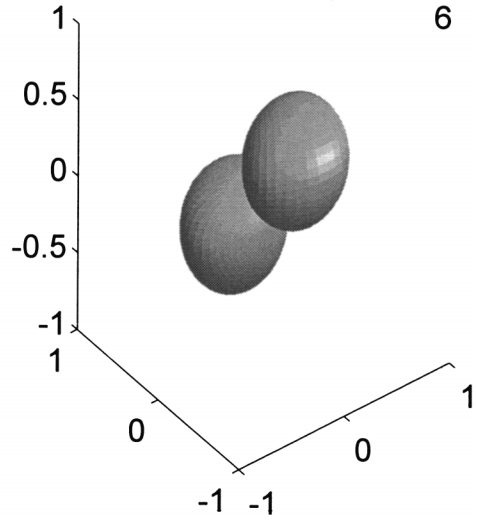
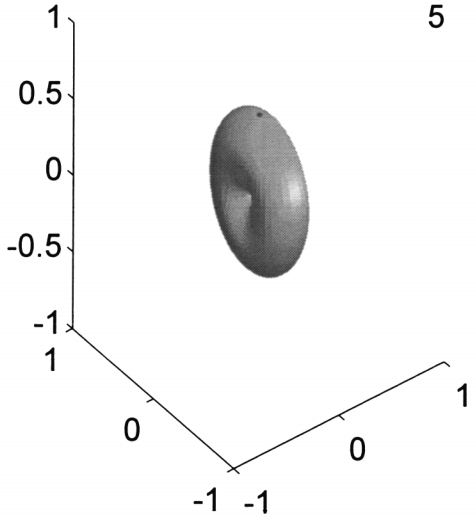
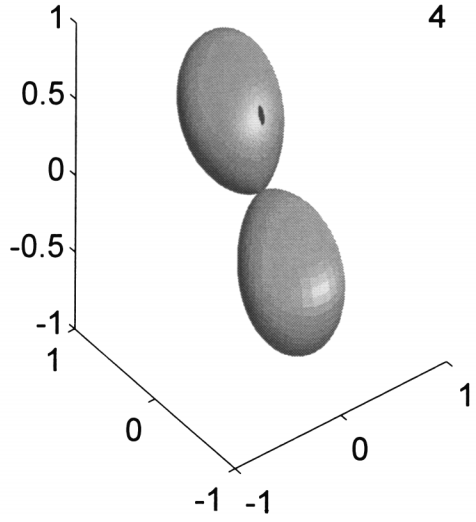
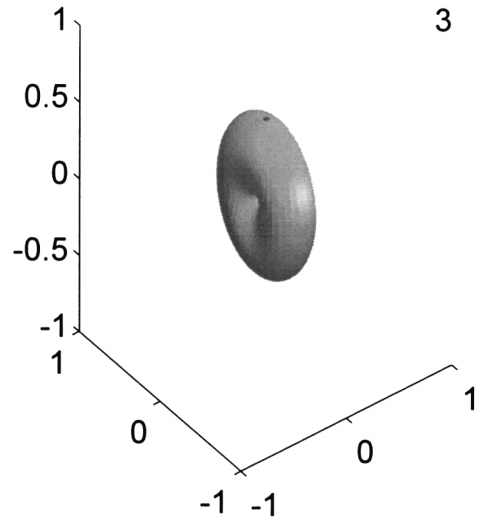
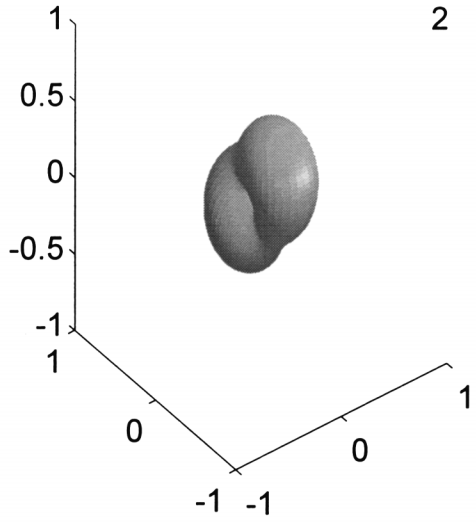
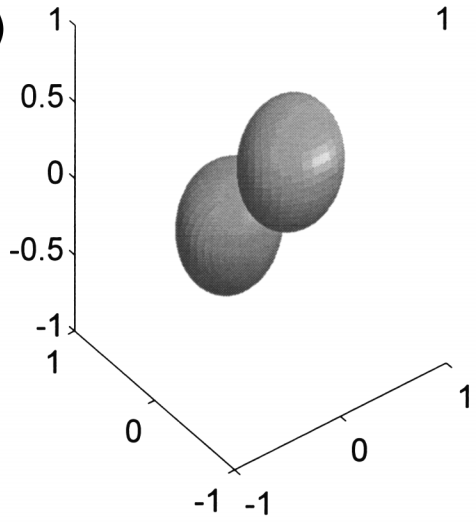
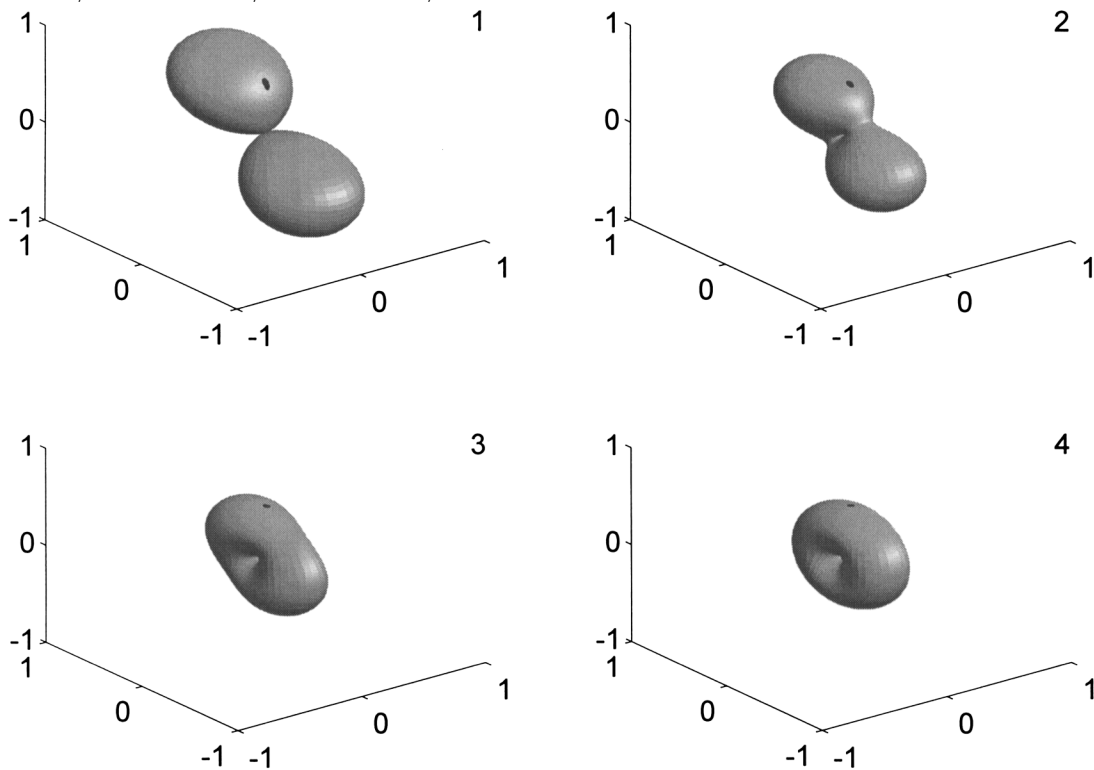


**Fig. 9.** Excitation with a continuous radiation of a  $J'' = 0 \rightarrow J' = 1$  transition in an electric field; 1 -  $\omega_\varepsilon/\Gamma = 0$ ; 2 -  $\omega_\varepsilon/\Gamma = 1.0$ ; 3 -  $\omega_\varepsilon/\Gamma = 2.5$ ; 4 -  $\omega_\varepsilon/\Gamma = \infty$ .



For this reason, we choose the excitation geometry where the  $\mathbf{E}$ -vector of the light has direction characterized by angles  $\theta = \pi/4$ ,  $\varphi = \pi/2$ , see Fig. 8a.

In this geometry, according to (14), the unit vector along the direction of light polarization has the following components:  $E^{+1} = i/2$ ;  $E^0 = 1/\sqrt{2}$ ;  $E^{-1} = i/2$ . This means that all three magnetic sublevels of the state  $J' = 1$  will be excited coherently. Keeping in mind that we still have a simple case because the transition probabilities characterized by Clebsch–Gordan coefficients are equal for all three transitions, we can write the total wave function as

$$\begin{aligned} \Psi_{J'}(t) &= e^{-i(E_0/\hbar)t} \sum_q E^q Y_{1q} e^{-i(E_M/\hbar)t} \\ &= e^{-i(E_0/\hbar)t} \left[ \frac{i}{2} \frac{1}{2} \sqrt{\frac{3}{2\pi}} \sin\theta e^{-i\varphi} e^{-i(E_{-1}/\hbar)t} + \frac{1}{\sqrt{2}} \frac{1}{2} \sqrt{\frac{3}{\pi}} \cos\theta e^{-i(E_0/\hbar)t} \right. \\ &\quad \left. + \frac{i}{2} \left(-\frac{1}{2}\right) \sqrt{\frac{3}{2\pi}} \sin\theta e^{i\varphi} e^{-i(E_1/\hbar)t} \right] \end{aligned} \quad (24)$$

We now assume  $E_M$  has the form of (21) (quadratic Stark effect) and pulse excitation. Then we have the evolution of quantum probability density in the case of Stark quantum beats

$$|\Psi_{J'}(t)|^2 \sim 1 - \sin^2\theta \cos^2\varphi + \sin 2\theta \sin\varphi \cos\Delta\omega t \quad (25)$$

where  $\Delta\omega$  is a splitting between sublevels  $M_J = \pm 1$  (degenerated) and  $M_J = 0$ . The evolution of  $|\Psi_{J'}(t)|^2$  appears to be cyclic. One period of this evolution is shown in Fig. 8b. We see now that—

contrary to magnetic quantum beats—the shape of the probability density changes and is restored only after half a period, although in a different orientation in space. After a full period, the orientation in space is restored. We see that for  $J \sim 1$  we have Stark quantum beats that disappear in a large  $J$  limit, see (19). With increase in  $J$  the period of restoration of the initial  $|\Psi_J(0)|^2$  distribution increases until at the  $J \rightarrow \infty$  limit beats disappear [14]. This has a simple explanation. At the limit  $J \rightarrow \infty$ ,  $\tilde{\omega}_0 \sim J^{-4}$  and the smallest frequency  $\omega_{MM+\Delta M}$  between coherently excited sublevels, which determine the quantum beat period at the limit  $J \rightarrow \infty$ , approaches zero and as a result the period increases infinitely and beats disappear.

Now, we can also calculate the Hanlé-type behavior of the probability density at stationary excitation. To this end, we need to find the time average of (25) multiplied by the decay factor  $\exp(-\Gamma t)$  and we obtain

$$\overline{|\Psi_{J'}(t)|^2} \sim \frac{1}{\Gamma} (1 - \sin^2 \theta \cos^2 \varphi) + \frac{\Gamma}{\Gamma^2 + \Delta\omega^2} \sin 2\theta \sin \varphi \quad (26)$$

In Fig. 9 this distribution is depicted as dependent on parameter  $\chi = \Delta\omega/\Gamma$ .

Besides the effects described above, an electric field can, in general, mix together wave functions  $Y_{JM}$  with the same value of  $M$ , but different  $J$ . However, if the distance in energy scale between quantum states with different  $J$  is large in comparison to the energy  $d\mathcal{E}$ , it may be neglected [13].

The main peculiarity of this distribution is the fact that at a high electric field limit  $\Delta\omega \rightarrow \infty$ , we still have distributions that have no axial symmetry with respect to the external field  $\mathcal{E}$ . This may seem strange. We are used to situations where the external field symmetrizes the distribution in the plane perpendicular to the direction of the field. In spectroscopy, this leads to the total depolarization of fluorescence if viewed from the end of the external field. We had exactly this situation in the previous examples in a magnetic field. Nevertheless, there is a simple explanation for this peculiarity.

In our last example, we had three pairs of coherently excited sublevels, namely,  $|11\rangle - |10\rangle$ ,  $|1-1\rangle - |10\rangle$ , and  $|1-1\rangle - |11\rangle$ . Only the coherence between the first two pairs can be destroyed by an external field by increasing their separation in energetic scale. The sublevels of the last, the third pair, are degenerated and remain so at any field strength. This means that coherence between these sublevels is preserved, and it can be shown [2] that this means anisotropic distribution in a plane perpendicular to the direction of the external field  $\mathcal{E}$ .

#### 4. Quantum-mechanical density matrix and classical probability density description of angular-momentum dynamics

The last two examples where we derived a superpositional wave function for the state  $J' = 1$  created in an optical transition  $J'' = 0 \rightarrow J' = 1$  (see (24)) show how complicated the wave function will look for the transition where  $J'' \sim 100 \rightarrow J' \sim 100$  ( $J'' - J' = 0, \pm 1$ ). We then have  $2J' + 1$  excited-state sublevels. A coherent superposition of these substates is created in an optical absorption from  $2J'' + 1$  ground-state sublevels. Usually, the quantum density-matrix formalism is used [15] to cope with all these substates. In the simplest case, the density-matrix elements can be written as [7]

$$f_{MM'} = a_M a_{M'}^* \quad (27)$$

where  $a_M$  and  $a_{M'}$  are the coefficients showing the part of  $Y_{JM}$  in the total wave function  $\Psi_J$ , say, for  $Y_{11}$  in (24) the coefficient is  $a_{+1} = (1/2) \exp\{-i[(E_0 + E_{+1})/\hbar]t\}$ . Methods were developed to calculate the density matrix  $f_{MM'}$  elements for definite experimental conditions.

In the more general case where atoms or molecules are excited with low intensity radiation, the density-matrix elements can be calculated as follows: [1]

$$\dot{f}_{MM'} = \langle M | \hat{d}\hat{E}^* | \mu \rangle \langle M' | \hat{d}\hat{E}^* | \mu \rangle^* - \Gamma f_{MM'} - i\omega_{MM'} f_{MM'} \quad (28)$$

where  $\hat{d}$  is the transition dipole moment operator, but  $\omega_{MM'} = (E_M - E_{M'})/\hbar$ . Furthermore, we can write

$$\langle M | \hat{d} \hat{E}^* | \mu \rangle = \Gamma_p \sum_q (E^q)^* C_{J'\mu 1q}^{JM} \quad (29)$$

where  $C_{\alpha\alpha b\beta}^{c\gamma}$  is the Clebsch–Gordan coefficient, and the proportionality coefficient  $\Gamma_p$  is called the *pumping rate*.

If all density-matrix elements are known, we are now able to calculate the quantum probability density

$$|\Psi_J|^2 = \sum_{MM'} f_{MM'} Y_{JM} Y_{JM'}^* \quad (30)$$

However, for states with large  $J$  it is a complicated task. There are no tables of explicit analytical expressions for  $Y_{JM}$  for large  $J$ ; the only thing we have at hand are recursion relations [9].

However, a couple of years ago, a method was developed that allowed an easy transition to be made from the quantum density matrix  $f_{MM'}$  to a classical probability density  $\rho(\theta, \varphi)$  for angular momentum. It can be shown that the density-matrix elements  $f_{MM'}$  at the  $J \rightarrow \infty$  limit can be considered as coefficients of the Fourier expansion of a classical probability density  $\rho(\theta, \varphi)$  [3, 16]

$$\rho(\theta, \varphi) = \sum_{\mu=-\infty}^{\infty} e^{-i\mu\varphi} f_{M+\frac{\mu}{2}, M-\frac{\mu}{2}}, \quad \cos\theta = \frac{M}{\sqrt{J(J+1)}} \quad (31)$$

The last equation is not restricted to the case where we have a coherent superposition of two  $M$  states belonging to the same  $J$ . If they belong to different  $J$  states, all we have to do is replace  $J$  with  $(J_1 + J_2)/2$ . The reciprocal to (31) can be written as

$$f_{M+\frac{\mu}{2}, M-\frac{\mu}{2}} = \frac{1}{2\pi} \int_0^{2\pi} e^{i\mu\varphi} \rho(\theta, \varphi) d\varphi \quad (32)$$

In practice, we almost always have the situation where values of  $\mu$  when  $f_{M+\frac{\mu}{2}, M-\frac{\mu}{2}}$  differs from zero are small in comparison to the interval of all allowed  $M$  values. For most cases of practical interest it makes the calculus of (31) rather simple.

Let us consider some examples of how to pass from  $f_{MM'}$  to  $\rho(\theta, \varphi)$  and to visualize in this way the results of quantum calculations at the large- $J$  limit.

The simplest case is when we excite the  $Q$ -type molecular transition with light linearly polarized along the  $z$  axis. In this case, only the diagonal elements of  $f_{MM}$  differ from zero

$$f_{MM} = (C_{JM10}^{JM})^2 = \frac{M^2}{J(J+1)} \quad (33)$$

For details of the calculation of the density-matrix elements, see ref. 17.

For the example considered in (31) only one summand is left. If we replace  $M$  by  $\sqrt{J(J+1)} \cos\theta$  according to (31), we immediately get

$$\rho(\theta, \varphi) = \cos^2\theta \quad (34)$$

To this end, we do not even need to consider an  $J \rightarrow \infty$  transition. Expression (34) is a precise result of (31) for any  $J$  value! From the viewpoint of classical physics at a large- $J$  limit, this result is of course obvious, see Sect. 2.1.



As a further example, let us consider the  $Q$ -type excitation without external fields at the geometry where the polarization vector of the light is along the  $y$  axis. We have then

$$f_{MM} = \frac{1}{2} \left[ (C_{JM-1\ 11}^{JM})^2 + (C_{JM+1\ 1-1}^{JM})^2 \right] = \frac{J(J+1) - M^2}{2J(J+1)} \quad (35)$$

$$\begin{aligned} f_{M+1,M-1} = f_{M-1,M+1} &= \frac{1}{2} C_{JM-1\ 1-1}^{JM-1} C_{JM\ 11}^{JM+1} = -\frac{\sqrt{(J^2 - M^2) [(J+1)^2 - M^2]}}{2J(J+1)} \\ &\approx -\frac{J(J+1) - M^2}{2J(J+1)} \end{aligned} \quad (36)$$

The explicit expressions for the Clebsch–Gordan coefficients can be found in refs. 1, 8, and 9. Inserting these  $f_{MM'}$  in (31), we get three summands allowing us to easily obtain

$$\rho(\theta, \varphi) = \sin^2 \theta \sin^2 \varphi \quad (37)$$

a result we already have in the pure classical approach, see (5) and (19), when  $\omega_B = 0$  and  $\tilde{\omega}_E = 0$ . In the same way, by considering  $f_{MM'}$  elements in the presence of an external field (directed along the  $z$  axis) in the geometry of the previous example, we obtain for the molecular transition  $J'' \rightarrow J'$  (see ref. 1 (5.12))

$$f_{MM} \sim \frac{1}{\Gamma} \frac{1}{2} \left[ \left( C_{J''M-1\ 11}^{J'M} \right)^2 + \left( C_{J''M+1\ 1-1}^{J'M} \right)^2 \right] \quad (38)$$

$$f_{M-1\ M+1} \sim \frac{1}{\Gamma + i\omega_{M-1\ M+1}} \frac{1}{2} C_{J''M-1\ 1-1}^{J'M-1} C_{J''M\ 11}^{J'M+1} \quad (39)$$

$$f_{M+1\ M-1} \sim \frac{1}{\Gamma + i\omega_{M+1\ M-1}} \frac{1}{2} C_{J''M\ 11}^{J'M+1} C_{J''M-1\ 1-1}^{J'M-1} \quad (40)$$

If we write  $\omega_{M\mp 1\ M\pm 1} = (E_{M\mp 1} - E_{M\pm 1})/\hbar$  in explicit form using  $E_M$  formulas of the type (7) and (21) or more complicated ones for special cases, after manipulations similar to those in the previous example, we can obtain from quantum-mechanical calculations  $\rho(\theta, \varphi)$  dynamics in an external field at the  $J \rightarrow \infty$  limit. This method allows us to visualize the angular-momentum distribution.

It may seem that the approach in which we perform the transition from the  $f_{MM'}$  description to the  $\rho(\theta, \varphi)$  description does not provide new results. As demonstrated in the previous sections, all these results (at least in a case of a simple  $E_M$  dependence on  $M$  and external field) can be obtained directly from the classical approach. However, this is not always the case. This will be proved in the last example.

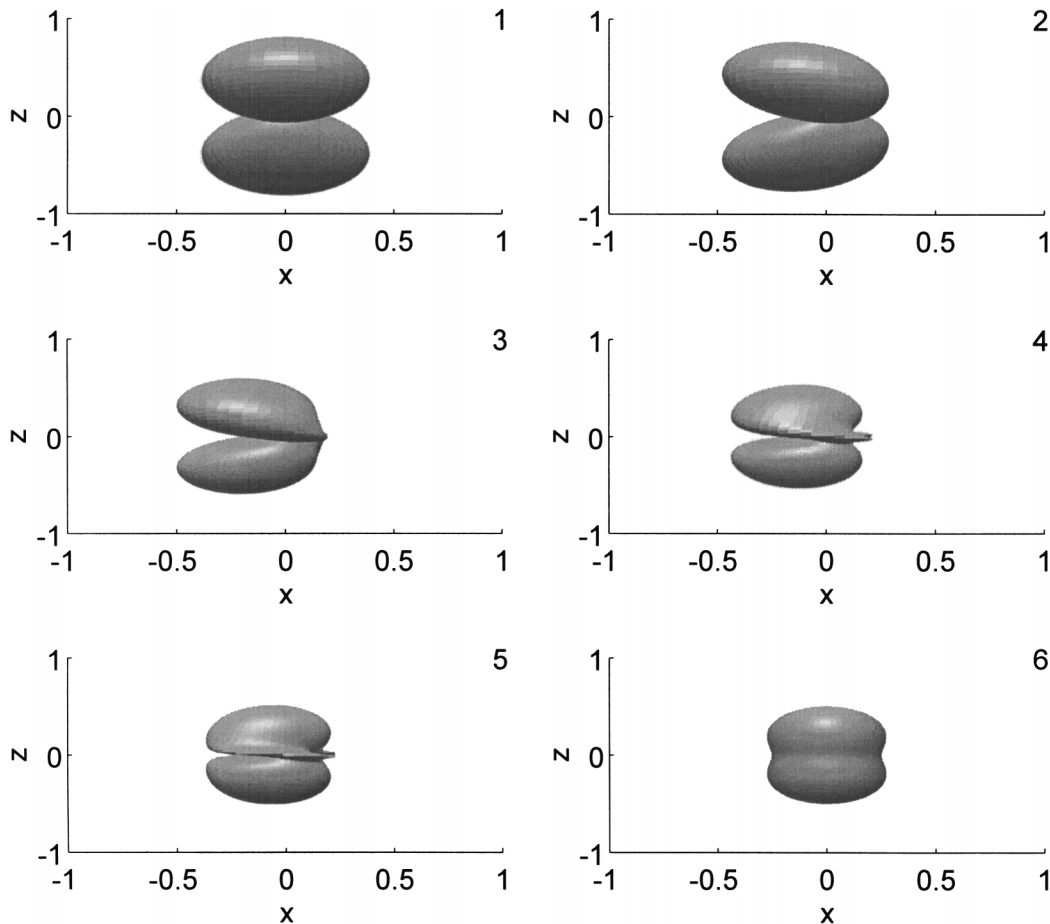
Usually, when exciting the ensemble of particles with linearly polarized light we expect that the fluorescence will also be linearly polarized, i.e., under different perturbations we expect the initially aligned ensemble (that can readily be illustrated by a double-pointed arrow  $\Leftarrow\Rightarrow$ ) of particles to change the actual shape of its angular momentum distribution, but to remain aligned. In other words, no orientation (that may be illustrated by a single-pointed arrow  $\Rightarrow$ ) will occur.

However, there are some kind of perturbations, and among them an influence on the external electric field, that can cause an alignment–orientation conversion. The conditions necessary to cause such a transition in general are analyzed in refs. 17 and 18.

The phenomenon itself is sometimes considered counterintuitive, and in this case this is why it is especially interesting to visualize the dependence of  $\rho(\theta, \varphi)$  on the strength of an external field.

Let us consider once more the excitation of an ensemble of molecules in an external electric field  $\mathcal{E}$  in the geometry of Fig. 8a. This time, we consider the  $Q$ -type absorption in the  $J \rightarrow \infty$  limit.

**Fig. 10.** Alignment–orientation conversion caused by a quadratic Stark effect; 1– $\chi = 0$ ; 2– $\chi = 0.5$ ; 3– $\chi = 2$ ; 4– $\chi = 4$ ; 5– $\chi = 8$ ; 6– $\chi = \infty$ .



Using (28) and (29), the explicit form of the Clebsch–Gordan coefficients [1, 9], and replacing  $M$  with  $\sqrt{J(J+1)} \cos \theta$  for nonzero density-matrix elements in this limit, we get

$$f_{MM} \approx \frac{1}{4} (1 + \cos^2 \theta) \quad (41)$$

$$f_{M\mp\frac{1}{2}, M\pm\frac{1}{2}} \approx \mp \frac{1}{4} \frac{1}{1 \pm i\chi \cos \theta} \sin 2\theta \quad (42)$$

$$f_{M\mp 1, M\pm 1} \approx -\frac{1}{8} \frac{1}{1 \pm i2\chi \cos \theta} \sin^2 \theta \quad (43)$$

where  $\chi = 6\tilde{\omega}_0 \mathcal{E}^2 / \Gamma$ .

Now, we have all we need to accomplish the transition to  $\rho(\theta, \varphi)$  according to (31). The result is

$$\rho(\theta, \varphi) = \frac{1}{4} (1 + \cos^2 \theta) - \frac{1}{2} \sin 2\theta \frac{\sin \varphi + \chi \cos \theta \cos \varphi}{1 + \chi^2 \cos^2 \theta} - \frac{1}{4} \sin^2 \theta \frac{\cos 2\varphi - 2\chi \cos \theta \sin 2\varphi}{1 + 4\chi^2 \cos^2 \theta} \quad (44)$$

The expression looks rather complicated unless a figure is drawn that illustrates graphically how  $\rho(\theta, \varphi)$  depends on  $\mathcal{E}$  or on the parameter  $\chi$ , see Fig. 10. Note, that in this figure the projection from

the end of the  $y$  axis is depicted. It allows us to demonstrate the effect of the alignment–orientation transition most effectively.

In a  $Q$ -type absorption in the absence of an external field, the angular-momentum distribution is in the shape of a “dumb-bell” lying along a light  $\mathbf{E}$ -vector; at  $\chi = 0$ , Fig. 10(1), we have a dumb-bell lying in the  $yz$  plane and tilted by  $45^\circ$  with respect to the  $z$  axis.

We see that the initial alignment by an electric field is transformed into a strong orientation (compare Figs. 10(1) and 10(3)). In Fig. 10(3), much more angular momentum is directed towards the negative  $x$ -axis end than towards the positive end. However, by increasing the field further, the orientation will again be destroyed.

The phenomenon can be easily explained from the classical model of the quadratic Stark effect, see Sect. 3.1. We remember that the angular momentum with the positive and negative projections on the direction of the electric field  $\mathcal{E}$  precesses in this field in the opposite direction. The initial distribution of the angular momentum has a symmetry that leads to the situation that both ends of the dumb-bell precess in opposite directions and at some particular electric field value are directed in the same direction, see Fig. 10(3). This is the creation of the orientation of the angular-momentum distribution.

This effect can be used to produce molecules with a particular orientation [19] as well as providing a sensitive method to measure different intramolecular interactions [20, 21].

Another way how to connect the quantum-mechanical density matrix  $f_{MM'}$  to the classical probability density  $\rho(\theta, \varphi)$  is by using multipolar expansion. We can expand  $f_{MM'}$  over the irreducible tensor operators  $T_Q^K$  [1, 15]

$$f_{MM'} = \sum_{K=0}^{2J'} \sum_{Q=-K}^K (-1)^Q f_Q^K (T_{-Q}^K)_{MM'} \quad (45)$$

This is a simple way of accounting for the symmetry properties of the processes that the particles are undergoing.

The direct analogy of (45) in classical physics is expansion of  $\rho(\theta, \varphi)$  over spherical functions  $Y_{KQ}$

$$\rho(\theta, \varphi) = (4\pi)^{-1/2} \sum_{K=0}^{\infty} \sum_{Q=-K}^K (2K+1)^{1/2} \rho_Q^K (-1)^Q Y_{KQ}^*(\theta, \varphi) \quad (46)$$

It means that if we have calculated in the quantum-mechanical approach multipolar moments  $f_Q^K$  for any particular problem in the limit  $J \rightarrow \infty$  we can obtain a classical angular-momentum distribution just by replacing the classical multipolar moments  $\rho_Q^K$  in expression (46) by the respective quantum multipolar moment  $f_Q^K$ . This method with numerous examples is discussed in great detail in refs. 1 and 2 and I will not go into further details here.

## 5. Concluding remarks

The aim of this paper was to examine the relationship between the classical and quantum descriptions of the angular-momentum distribution in an ensemble of particles.

As was demonstrated in this paper, there is more in common between the quantum and classical descriptions of angular moments, than can be seen at first glance. In Sects. 2.1 and 2.2 it was shown that not only does the angular momentum  $J$  precess in an external field in classical physics, but we can also associate it with a “precession” of the quantum-mechanical wave function in an external field, which is related to specific changes of the wave-function phase on the action of the field. The

importance of the wave-function phase is stressed and some examples of coherent superposition of states are presented.

If we perform the transition to the classical limit in quantum mechanics by setting  $J \rightarrow \infty$  in quantum equations for angular momenta, then we can obtain not only the same values for observable signals, such as we get from classical physics, but also the angular-momentum distribution function in both cases evolve similarly. Using the method we have discussed we can obtain the evolution of this distribution function in time as well as in space as a function of a stationary external field strength.

As an example, the interpretation of the Zeeman and Stark effects from the viewpoint of classical physics is presented and the influence of external magnetic and electric fields upon the angular-momentum distribution is discussed.

The method we describe to relate the quantum-mechanical density matrix  $f_{MM'}$  to the classical angular-momentum distribution function  $\rho(\theta, \varphi)$  helps one to better understand the results of quantum-mechanical calculations. It can help to interpret the results in terms of angular-momentum dynamics and to get a simple graphical explanation of the sometimes counterintuitive quantum results as was demonstrated in the case of the alignment–orientation transition.

## Acknowledgment

Support by the research group Interaction of Oriented Molecules of the Center for Interdisciplinary Research (ZiF) at the University of Bielefeld is gratefully acknowledged.

## References

1. M. Auzinsh and R. Ferber. Optical polarization of molecules. Cambridge University Press, Cambridge, U.K. 1995. p. 306.
2. M. Auzinsh and R. Ferber. Phys. Rev. A, **43**, 2374 (1991).
3. K.A. Nasyrov and A.M. Shalagin. Sov. Phys. JETP, **54**, 877 (1981).
4. W.J. Duffin. Electricity and magnetism. McGraw-Hill Book Co., London, New-York, Toronto, Sydney. 1965. p. 452.
5. G. Herzberg. Molecular spectra and molecular structure. I. Spectra of diatomic molecules. D. Van Nostrand Co., Princeton, New Jersey, Toronto, London, New York. 1957. p. 658.
6. D.A. Case, G.M. McClelland, and D.R. Herschbach. Mol. Phys. **35**, 541 (1978).
7. E.B. Alexandrov, M.P. Chaika, and G.I. Khvostenko. Interference of atomic states. Springer-Verlag, Berlin, Heidelberg, New York. 1993. p. 250.
8. R.N. Zare. Angular momentum. J. Wiley & Sons, New York. 1988. p. 280.
9. D.A. Varshalovich, A.N. Moskalev, and V.K. Khersonskii. Quantum theory of angular momenta. World Scientific, Singapore. 1988. p. 514.
10. J.P. Lowe. Quantum chemistry. Academic Press, New York, San Francisco, London. 1978. p. 599.
11. G. Moruzzi and F. Strumia. Hanlé effect and level-crossing spectroscopy. Plenum Press, New York, London. 1991. p. 371.
12. R.C. Hilborn. Am. J. Phys. **63**, 330 (1995).
13. W.H. Flygare. Molecular structure and dynamics. Prentice-Hall, New Jersey. 1978. p. 460.
14. M. Auzinsh, R. Ferber, and A.V. Stolyarov. J. Chem. Phys. **101**, 5559 (1994).
15. K. Blum. Density matrix. Theory and applications. Plenum Press, New York, London. 1981. p. 246.
16. M.P. Auzinsh, K.A. Nasyrov, M.Ya. Tamanis, R.S. Ferber, and A.M. Shalagin. Sov. Phys. JETP, **65**, 891 (1987).
17. M.P. Auzinsh and R.S. Ferber. J. Chem. Phys. **99**, 5742 (1993).
18. U. Fano. Phys. Rev. **133**, B828 (1964).
19. M.P. Auzinsh and R.S. Ferber. Phys. Rev. Lett. **69**, 3463 (1992).
20. P.I. Klincare, M.Ya. Tamanis, A.V. Stolyarov, M.P. Auzinsh, and R.S. Ferber. J. Chem. Phys. **99**, 5748 (1993).
21. M.P. Auzinsh, A.V. Stolyarov, M.Ya. Tamanis, and R.S. Ferber. J. Chem. Phys. **105**, 37 (1996).